Enhanced self-healing using conventional supplementary cementitious materials

R. Maddalena, D. Gardner
School of Engineering, Cardiff University, UK

H. M. Taha
Department of Architecture & Civil Engineering, University of Bath, UK

ABSTRACT
Crack formation is one of the main causes of deterioration in cement and concrete. Cracks in the cover zone lead to fluid ingress and subsequent modification of the pH of the cement matrix. This, in turn may result in disruption to the passive film that protects steel reinforcement, the onset of rust formation and the overall safety of a concrete element being compromised.

In this work, we present a comparison between cement mortar mixes using ordinary Portland cement (CEM I) with different replacements of supplementary cementitious materials typically used in the construction industry: silica fume, ground granulated blast-furnace slag (GGBS) and pulverised fuel ash (PFA). Samples were subjected to mechanical damage to open micro-cracks and then placed in a healing bath to trigger autogenous self-healing. The latter occurs via the additional formation of calcium (aluminium) silicate hydrates (C-(A)-S-H) due to further hydration of the starting reactants. Micro-structure characterisation analysis, powder X-Ray diffraction (XRD) and thermogravimetric analysis (TGA/DSC) were used to identify and quantify the hydration products pre- and post-healing. Pore structure and physical property measurements (i.e. open porosity, density, water absorption and sorptivity) were used to determine the effectiveness of the self-healing process in reducing crack-widths and recovering the water-tightness of the mortar matrix post-healing.

1. INTRODUCTION

Crack formation in cementitious building materials is a common phenomenon, which can occur either on the surface or inside structural elements. Cracks are often related to a structure's deterioration as they facilitate water ingress, hence triggering reinforcement depassivation leading eventually to reinforcement corrosion (Liu and Shi, 2011). The exposure of pores containing water and salts to a temperature gradient may result in crystallisation of the salts, the expansive nature of which is sufficient to induce microcracking in the cement matrix (Espinosa-Marzal et al., 2011).

A number of technologies have been studied and developed to prevent cracks formation or to provide cracks closure. So-called self-healing concrete provides a solutions to repair cracks at different scales. Micro-cracks could be sealed by adding microcapsules that contain a healing agent into the fresh paste (Ferrara et al., 2018). Recently, bacteria have also been used as a crack healing technique via the inclusion of bacteria spores and nutrients in the fresh paste. The formation of cracks allows water to penetrate into the cementitious matrix, therefore stimulating the bacteria to precipitate calcium carbonate using the calcium hydration products which are already present in hydrated concrete (i.e. portlandite($Ca(OH)_2$)). The precipitation of calcium carbonate from this process contributes to crack blockage (Wang et al., 2014). Other researchers examined external intervention methods for healing damage. (Gardner et al., 2017) investigated the self-healing capability of flowing healing-liquid agents (i.e. cyanoacrylate) into hollow channels within cement and concrete specimens. Cracks can be mechanically closed as well by using shape memory polymers tendons, placed in concrete elements during casting. At the onset of a crack, the tendons are heated to trigger the shape memory effect and close the crack by exerting a compressive force across the crack plane (Teall et al., 2017).

Self-healing properties of fibre reinforced cement using plastic fibres (e.g. polyvinyl alcohol, polypropylene, etc) have been investigated (Nishiwaki et al., 2014). The fibres act as crack-bridges and their high specific surface area offer additional nucleation and growth sites for the formation and precipitation of further hydration products.

Supplementary cementitious materials (SCM) are industrial by-products (e.g. manufacturing industry, excavation and mining sites etc.). Their amorphousness and elevated specific surface area provide a nucleation site for the formation of calcium silicate hydrate (C-S-H) from unreacted reactants. The usage of SCM as cement replacement is regulated by international standards, and their usage is widely encouraged as a viable environmental friendly solution.

In this study we investigated the self-healing capability of mortar cement partially replaced by silica fume, pulverised fuel ash and grounded

1

granulated blast-furnace slag. Further hydration and additional formation of hydrated minerals is evaluated by water transport properties and thermal and mineralogical analysis.

2. MATERIALS AND METHODS

Cement mortar was prepared using ordinary Portland cement CEM I (strength class 52.5 MPa), silica sand, at sand to binder ratio (s/b) of 3, and deionized water at water to binder ratio (w/b) of 0.45. Portland cement was partially replaced by supplementary cementitious materials (SCM) at different percentages. Commercially available SCMs were used; amorphous silica fume (SF), ground granulated blast-furnace slag (GGBS) and pulverized fuel ash (PFA). Samples and replacement proportions are reported in Table 1. The percentage of replacement was chosen in agreement to the highest content allowed by BS EN197.

Table 1. Sample ID name and mixing proportions of cement replacement using silica fume (SF), pulverised fuel ash (PFA) or ground granulated blast-furnace slag (GGBS).

Sample name	OPC (%)	SF (%)	PFA (%)	GGBS (%)
OPC	100	-	-	-
S	90	10	-	-
P	70	-	30	-
B	50	-	-	50

Mortar paste was mixed according to the BS EN 196-1 and cast into steel moulds of 25 x 25 x 25 mm. After 24 hours specimens were demoulded and cured for 28 days in a sealed environment at 95% relative humidity and 20 °C to prevent carbonation (Cerveny et al., 2011).

After curing, the samples were gently oven-dried at 55 °C until no further change in weight was recorded (Zhang and Scherer, 2011). Specimens were then subjected to mechanical damage, using a uniaxial loading cell with a load up to 90% of the maximum peak before failure, to cause micro-cracks and internal damage. The cubes were then placed in a static healing bath of deionised water to promote further hydration and crack-healing.

Physical characteristics and water transport properties (sorptivity) were measured in (u) undamaged conditions (after curing), (d) damaged conditions (after mechanical loading and micro-cracking), and (h) healed conditions (after 60 days in deionised water).

Mineral composition by means of X-ray diffraction measurements and thermogravimetric analysis were conducted on samples at damaged (d) and healed (h) conditions.

The sorptivity test measures the water uptake through the capillary rise effect in the pore structure with time. The test was used to determine the healing capability of the different mixes. For each mix, three samples were used. The samples were placed in a container with 1 mm of their bottom surface in contact with deionised water. The water uptake was measured indirectly through the sample weight increase with time, over a period of 100 minutes at defined intervals. The methodology was adapted from the HAMSTAD Round Robin test method (Ioannou, Hamilton and Hall, 2008). The same test method was followed to perform open porosity measurements, bulk density and matrix density on three specimens for each mix, at each stage ((u), (d) and (h)).

Powder X-ray diffraction patterns were collected from 5° to 60° 2θ at a rate of 1°/min and a step size of 0.02 °2θ.

Thermal analysis were used to quantify mineral phases due to the healing process and further hydration. TGA/DSC curves were collected from 25 °C to 1000 °C at a heating rate of 10 °C/min under constant nitrogen flow. The mass loss was calculated using the tangent method (Matschei, Lothenbach and Glasser, 2007) at three different temperature ranges; 90-150 °C, temperature range of pore-water evaporation, and the decomposition of both C-S-H and ettringite; 440-440 °C, dehydroxilation of portlandite and 660-700 °C, decomposition of carbonated products (Maddalena, Hall and Hamilton, 2019). TGA mass loss at the specific temperature range was used to estimate the mineral phase relative content on damaged samples, condition (d), and healed samples, condition (h).
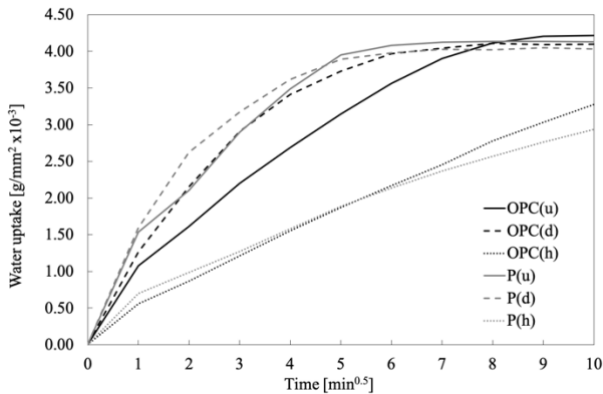
3. RESULTS AND DISCUSSION

The physical characteristics of the different mixes are reported in Table 2. The porosity and the density values are typical of mortar and concrete matrices. The pore volume, measured as open porosity (ϕ) and the material density values (bulk and matrix density) are constant throughout the three stages (undamaged, damaged and healed). The water uptake after 100 minutes decreased by ca. 24% in sample OPC, and by ca. 50% in sample S, P and B, with 10%, 30% and 50% replacement of SF, PFA and GGBS respectively. The measurement of open porosity provides an estimate of the accessible pore volume but does not take into account pores with an average diameter at the micro-scale.

Table 2. Average values of open porosity (ϕ), bulk density (ρ), matrix density (ρ_{mat}), and water uptake at 100 minutes (W_{100}) in undamaged (u), damaged (d) and healed (h) conditions.

Sample name		ϕ (%)	ρ (g/cm^3)	ρ_{mat} (g/cm^3)	W_{100} (g/mm^{2}10^{-3})
OPC	(u)	0.18	2.05	2.49	4.2
	(d)	0.18	2.03	2.47	4.1
	(h)	0.19	2.03	2.51	3.3
S	(u)	0.17	2.02	2.44	4
	(d)	0.18	2.01	2.43	3.7
	(h)	0.19	2.00	2.46	2
P	(u)	0.19	2.01	2.46	4.1
	(d)	0.19	2.02	2.49	4
	(h)	0.20	2.02	2.51	2.9
B	(u)	0.18	2.01	2.46	4.5
	(d)	0.18	2.00	2.46	4.3
	(h)	0.19	2.01	2.48	2.9

Conversely, the reduction in water uptake (W_{100}) suggested that self-healing due to further hydration

took place most probably in the micro-pores. The sorptivity curves for OPC and sample P are reported in Figure 1.
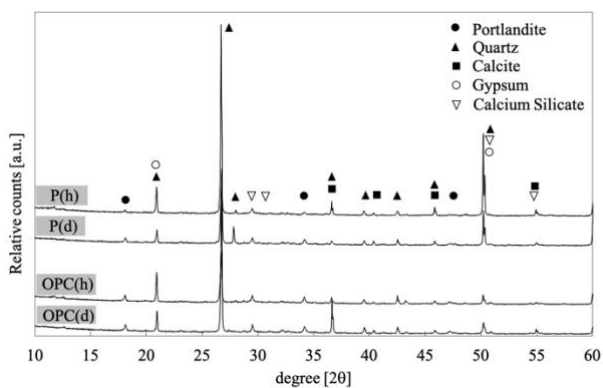

Figure 1. Water uptake recorded during sorptivity measurements for sample OPC and sample P (30% replacement of PFA) as a function of time, in undamaged (d), damaged (d) and healed (h) conditions.

While the water uptake values at 100 min are similar for undamaged (u) and damaged (d) conditions due to the size of the sample, their slope is different in the two cases. The decreased rate of water absorption in samples OPC(h) and P(h) shows the effect of further hydration, reducing the pore volume and crack spacing by formation of C-S-H or calcium carbonate.

The formation of C-S-H is balanced by a reduction in portlandite, naturally present in hydrated cement paste, since silica reacts with $Ca(OH)_2$ and water to form C-S-H.
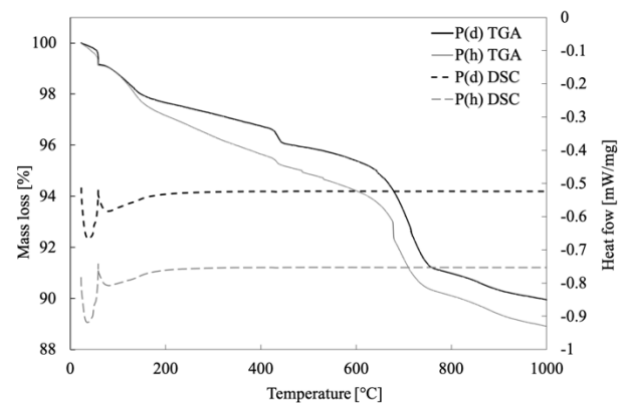
XRD patterns of sample OPC damaged (d) and healed (h), and sample P (30% PFA) damaged (d) and healed (d) are shown in Figure 2. The peaks at ca. 18°, 34° and 47° 2θ are the reflection of Portlandite crystals. A reduction in intensity is observed, suggesting that portlandite was consumed to form additional C-S-H. The patterns showed also an increase in intensity of the peaks associated to C-S-H, at ca. 29°, 32°, 50° and 55° 2θ.

Figure 2. X-Ray diffractogram of sample OPC and sample P after mechanical damaging (d) and after 60 days in healing bath (h). [Only the major mineral phases are indicate].
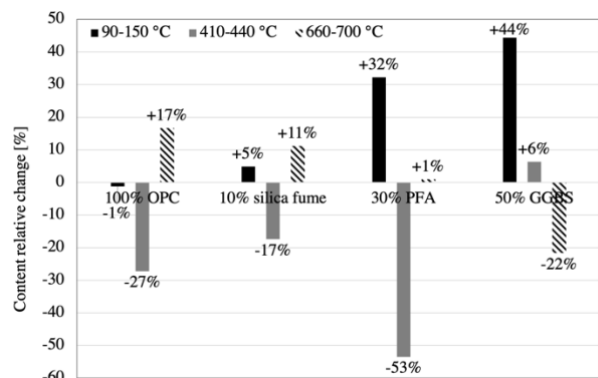
Further evidence of C-S-H formation, followed by a reduction in portlandite is shown in Figure 3. Thermogravimetric (TG) curves and differential

scanning calorimetry (DSC) response are reported for sample P (30% PFA) damaged (d) and healed (h). In this graph, downward DSC peaks indicate exothermic reactions, while upwards peaks indicate an endothermic reaction. In case of OPC replacement by PFA, we found that an increase weight loss in the temperature range 90-150 °C, associated to evaporation of pore water and dehydration of C-S-H, indicated a higher amount of C-S-H present in the sample P(h) in agreement with (Garbev *et al.*, 2008). The formation of C-S-H is possible because of the consumption of portlandite, as shown in the thermal step 410-440 °C (Maddalena and Hamilton, 2017). The relative mass loss change, between damaged (d) and healed (h) conditions, calculated for all the mixes (OPC, S, P and GGBS) at each thermal step is reported Figure 4.

Figure 3. Thermogravimetric analysis (TGA) and differential scanning calorimetry measurements for sample P (30% replacement of PFA) in damaged (d) and healed (h) conditions. [TGA: continuous line. DSC: dashed line].

The additional formation of C-S-H is more significant in sample mixed with PFA and GGBS. This is due to their chemical composition and their high pozzolanic reactivity. Samples prepared with GGBS showed an increase in C-S-H by ca. 44% and a reduction in calcium carbonate by 22%.

Silica fume samples did not show a significant increase in C-S-H (5%) but rather an increase in carbonated products, balanced by a reduction in portlandite (-17%).

Figure 4. Phase content relative change (at damaged and healed conditions) calculated from TGA loss mass measurements at three different temperature ranges, 90-150 °C, 410-440 °C and 660-700 °C respectively.

The water absorption rate for the silica fume however, showed a similar behaviour to the other mixes (PFA and GGBS), suggesting that silica fume improved the self-healing through its physical filling effect (Quercia *et al.*, 2012). Finally, the mix with PFA resulted in a higher reduction of portlandite (-53%) and an increase of C-S-H of ca. 32%.

4. CONCLUSIONS

This work investigated the self-healing capability of OPC mortar mixes partially replaced by 10% of silica fume, 30% PFA, and 50% GGBS. it has been found that the reactivity of SCM mixes promoted the formation of additional calcium silicate hydrate (C-S-H) which decreases their water absorption rate by ca. 50%.

The results showed that each SCM promoted the self-healing through different mechanisms (specific surface area, chemical composition, pozzolanic reactivity), indicating that ternary replacement combining different percentages of SF, PFA and GGBS could further enhance the self-healing capability of cementitious materials.

Further work will investigate the pore size distribution at the micro-scale using mercury intrusion porosimetry (MIP) measurements. Scanning electron microscopy will be also used to characterise the healing products in cracks and pores.

ACKNOWLEDGEMENT

REFERENCES

Cerveny, S. *et al.* (2011) 'Effect of hydration on the dielectric properties of C-S-H gel', *The Journal of Chemical Physics*. AIP Publishing, 134(3), p. 034509. doi: 10.1063/1.3521481.

Espinosa-Marzal, R. M. *et al.* (2011) 'The chemomechanics of crystallization during rewetting of limestone impregnated with sodium sulfate', *Journal of Materials Research*, 26(12), pp. 1472–1481. doi: 10.1557/jmr.2011.137.

Ferrara, L. *et al.* (2018) 'Experimental characterization of the self-healing capacity of cement based materials and its effects on the material performance: A state of the art report by COST Action SARCOS WG2', *Construction and Building Materials*. Elsevier Ltd, 167, pp. 115–142. doi: 10.1016/j.conbuildmat.2018.01.143.

Garbev, K. *et al.* (2008) 'Cell dimensions and composition of nanocrystalline calcium silicate hydrate solid solutions. Part 1: Synchotron-based X-Ray Diffraction', *Journal of the American Ceramic Society*, 91(9), pp. 3005–3014. doi: 10.1111/j.1551-2916.2008.02601.x.

Gardner, D. *et al.* (2017) 'Capillary Flow Characteristics of an Autogenic and Autonomic Healing Agent for Self-Healing Concrete', *Journal of Materials in Civil Engineering*, 29(11), p. 04017228. doi: 10.1061/(ASCE)MT.1943-5533.0002092.

Ioannou, I., Hamilton, A. and Hall, C. (2008) 'Capillary absorption of water and n-decane by autoclaved aerated concrete', *Cement and Concrete Research*, 38(6), pp. 766–771. doi: 10.1016/j.cemconres.2008.01.013.

Liu, Y. and Shi, X. (2011) 'Ionic transport in cementitious materials under an externally applied electric field: Finite element modeling', *Construction and Building Materials*, 27(1), pp. 450–460. doi: 10.1016/j.conbuildmat.2011.07.019.

Maddalena, R., Hall, C. and Hamilton, A. (2019) 'Effect of silica particle size on the formation of calcium silicate hydrate (C-S-H) using thermal analysis', *Thermochimica Acta*. Elsevier, 672(August 2018), pp. 142–149. doi: 10.1016/j.tca.2018.09.003.

Maddalena, R. and Hamilton, A. (2017) 'Low-pressure silica injection for porosity reduction in cementitious materials', *Construction and Building Materials*, 134. doi: 10.1016/j.conbuildmat.2016.11.016.

Matschei, T., Lothenbach, B. and Glasser, F. P. (2007) 'Thermodynamic properties of Portland cement hydrates in the system CaO–Al2O3–SiO2–CaSO4–CaCO3–H2O', *Cement and Concrete Research*, 37(10), pp. 1379–1410. doi: 10.1016/j.cemconres.2007.06.002.

Nishiwaki, T. *et al.* (2014) 'Self-Healing Capability of Fiber-Reinforced Cementitious Composites for Recovery of Watertightness and Mechanical Properties', *Materials*, 7, pp. 2141–2154. doi: 10.3390/ma7032141.

Quercia, G. *et al.* (2012) 'Effects of amorphous nano-silica addition on mechanical and durability performance of SCC mixtures', in *International Congree on Durability of Concrete*.

Teall, O. *et al.* (2017) 'Development of high shrinkage polyethylene terephthalate (PET) shape memory polymer tendons for concrete crack closure', *Smart Materials and Structures*. IOP Publishing, 26(4), p. 045006. doi: 10.1088/1361-665X/aa5d66.

Wang, J. Y. *et al.* (2014) 'Self-healing concrete by use of microencapsulated bacterial spores', *Cement and Concrete Research*. Elsevier Ltd, 56, pp. 139–152. doi: 10.1016/j.cemconres.2013.11.009.

Zhang, J. and Scherer, G. W. (2011) 'Comparison of methods for arresting hydration of cement', *Cement and Concrete Research*, 41(10), pp. 1024–1036. doi: 10.1016/j.cemconres.2011.06.003.